

# Automated Pole-Selection: Proof-of-Concept & Validation

**Jeroen Lanslots, Bert Rodiers, Bart Peeters**

LMS International, TST Technology Deployment & Research  
Researchpark Z1, Interleuvenlaan 68, B-3001, Leuven, Belgium  
e-mail: [jeroen.lanslots@lms.be](mailto:jeroen.lanslots@lms.be)

## Abstract

System identification from measured MIMO data plays a crucial role in structural dynamics and vibro-acoustic system optimization. The most popular modelling approach is based on the “modal analysis” concept, leading to an interpretation in terms of eigenmodes, visualized in so-called stabilization diagrams. Typically, the number of modes is very high (often over 100), including modes with high damping and high modal overlap. Therefore, a key problem of the system identification process is the selection of the correct model order and related to this, the selection of valid system poles. So far, this has been a problem to be solved by human expert engineers. This paper presents a proof-of-concept of a completely automated modal analysis process. In doing so, this paper presents a benchmark test that will prove that the performance of the automated tool is equal to or better than the performance of human expert engineers and as such will receive confidence for usage.

## 1 Introduction

System identification [1] is a standard tool for the analysis of artificially or ambient excited vibrating structures. In modal analysis, a number of parameter estimation techniques such as LSCE and PolyMAX are used to estimate the parameters that identify a system correctly (Section 3). These so-called modal parameters are resonance frequencies, damping ratios and modal shapes. To reduce the bias on the estimates and allow the model to capture all relevant characteristics of the structure, the identification order is usually chosen quite high. However, the higher the model order is chosen, the higher number of estimated poles will be calculated. This results in the occurrence of so-called spurious or mathematical poles that do not represent the physical behavior of the structure.

The results of these calculations are presented in a so-called stabilization diagram from which stabilized modes can be picked. Such a diagram shows the evolution of frequency, damping, and mode/participation vectors as the number of modes is increased. The physical modes can then be seen as those modes for which the frequency, damping, and mode/participation vector values do not change significantly. This is exactly the task of assessing a stabilization diagram, and so far experienced engineers do this by hand.

To automate this, an intelligent rule-based technique was developed that analyzes the stabilization diagram by selecting only the physical poles. This technique is based on knowledge acquisition that is achieved by observing skilled engineers. It has the advantage that it is much faster, that less-experienced people have access to knowledge from expert engineers, and furthermore, the method is deterministic and does not depend on the parameter estimation method used to obtain the stabilization diagram.

With the latest generation parameter estimation methods, stabilization diagrams have been cleaned of a lot of the spurious poles. This opens the opportunity for automated pole selection methods to be included as the final step, hereby completely automating the modal analysis process. In section 4, a proof of concept will be given by a combination of standard LMS Test.Lab software and Windows Automation.

Section 6 reports on a benchmark test that seeks to determine the performance of the automated rule-base

intelligence method. In doing so, three groups have been created:

- expert engineers using implicit knowledge: hence expertise, and experience;
- non-expert engineers using explicit knowledge: they will be using the rules as they have been extracted in the knowledge acquisition process;
- the automated pole-selection method: using the same extracted rules.

To compare the quality of the resulting pole selections, a number of validation criteria, presented in section 5, will be used. Section 7 will present conclusions on the performance of the automated tool with respect to the performance of human novice and expert engineers.

## 2 Overview of existing pole-selection methods

With the increasing use of modal analysis as a standard tool by many, also less experienced, users, the strong need is expressed to automate the process. Researched solutions include estimation methods that are much more robust with respect to the appearance of spurious poles such as PolyMAX. Nevertheless, the route to automation still requires discrimination methods to distinguish physical from mathematical poles.

Probably, the most “natural” way is trying to capture the decisions that an experienced modal analyst takes, based on a stabilization diagram, by rules that can be implemented as an autonomous procedure. Examples of such rules can be found in [2, 3, 4]. The rule-based approach [2, 3] will be used for the benchmark test, and is further described in section 4.

The amount of pole information that can be provided in a stabilization diagram is in fact bounded by the ability of the human mind to interpret them at a glance. Automated procedures do not suffer from this constraint and the pole classification can be based on much more information. Therefore research is performed on additional criteria that describe the stability of a pole. A first set of criteria is generic (i.e. independent of the system identification technique) and looks for instance at the complexity of the modal vector [5, 6, 7]. As mathematical poles are often characterized by high complexity, this criterion is valid if real modes are expected (loosely, if the distribution of the damping mechanisms along the vibrating structure is similar to its mass and stiffness distribution). Another criterion to get confidence in a pole of an identified MIMO model is to verify whether the pole is still present if different SIMO or even SISO models are identified by selecting individual inputs or outputs from the data [3, 6, 8, 9].

Other pole validation criteria emerged in combination with specific system identification techniques. For instance in [10], the autonomous procedure heavily relies upon the “Consistent-Mode Indicator” which was presented as a byproduct of the Eigensystem Realization Algorithm (ERA) [11]. Based on the realization theory, ERA identifies a state-space model from impulse response functions. Very interesting are the stochastic pole validation criteria that were formulated in combination with frequency-domain maximum likelihood estimation [6, 7, 12, 13]. These stochastic criteria propagate the data uncertainty to features such as: uncertainty on pole estimate (large uncertainty may indicate a mathematical pole), pole-zero pairs (large amount of zeros within a certain confidence circle around a pole is an indication of a mathematical pole), pole-zero correlation coefficient (high correlation again indicates a non-physical origin of pole).

A final set of criteria was developed to operate in combination with subspace identification [3, 9, 14]: modal model reduction (the effect of removing a mode from the state-space model is studied, where a small effect may indicate a mathematical pole), relation between balanced and modal form (the energy interpretation of the states of a balanced model is heuristically transferred to the poles of the system, where “low-energy” poles are considered as non-physical), forced pole-zero cancellations (if the effect on the model of shifting a pole towards its closest zeros is limited, this was probably a mathematical pole).

Evidently none of the methods works in all cases: many of them may give unclear separation in case of low signal-to-noise ratios; some of them may fail to label a local or weakly excited pole as a physical one; the mode complexity indicators fail if the structure exhibits complex physical modes. However, combining multiple criteria by clustering techniques drastically improves the pole-discrimination capacity. For instance, in [6, 13] Fuzzy C-means clustering is used for this purpose: the result is a membership function value for each pole that indicates whether it belongs to the class of physical or mathematical poles.

Clustering techniques are also used to automatically interpret a classical stabilization diagram [15]. In such an approach, advanced extensions of the original Fuzzy C-means clustering technique are used to cluster poles in terms of frequency and damping. Based on the final cluster centers, the most stable poles are chosen. In addition, [15] presents Genetic Algorithms as a suitable technique that can be used to initialize the fuzzy clustering and/or perform a stand-alone clustering.

### 3 Parameter estimation methods

Because of the complexity of the structural dynamics identification problem, a large variety of dedicated modal parameter estimation methods were proposed over the years. In most methods, the raw input-output data are first processed into a non-parametric system description matrix, consisting of FRFs (Frequency Response Functions) or IRs (Impulse Responses), resulting in a significant data reduction and allowing the use and combination of non-simultaneously measured data. This also fits the test reality where the modal testing process is often separated in time (and location) from the actual analysis process.

The matrix of FRFs or IRs can then be used as input data to establish the parameters of a system model such as a frequency or time domain state-space model (referred to as Eigensystem Realization (ERA) [11] or Subspace Identification [16], due to the inherent SVD model reduction), or to directly identify the structural parameters of a model described by the constitutive equations (Direct Parameter Estimation [17]). Both approaches have been implemented in the time as well as in the frequency domain in many different algorithms.

Alternatively, model formulations can be used which directly exploit specific properties of the FRFs (or IRs). For example, the FRF and IR matrices can be expressed directly in terms of the modal parameters:

$$[H(j\omega)] = \sum_{r=1}^{N_m} \left( \frac{Q_r \{\psi\}_r \{\psi\}_r^t}{(j\omega - \lambda_r)} + \frac{Q_r^* \{\psi\}_r^* \{\psi\}_r^{*t}}{(j\omega - \lambda_r^*)} \right) \quad (1)$$

$$[h(t)] = \sum_{r=1}^{N_m} \left( Q_r \{\psi\}_r \{\psi\}_r^t e^{\lambda_r t} + Q_r^* \{\psi\}_r^* \{\psi\}_r^{*t} e^{\lambda_r^* t} \right) \quad (2)$$

where  $Q_r$ : modal scaling factor,  $\{\psi\}_r$ : modal vector  $r$ ,  $\lambda_r$ : system pole  $\sigma_r + j\omega_r$ ,  $\sigma_r$ : damping factor,  $\omega_r$ : damped natural frequency,  $[V] := [\{\psi\}_1 \dots \{\psi\}_N \{\psi\}_1^* \dots \{\psi\}_{N_m}^*]$ : modal vector matrix.

Directly solving equation (1) leads to the non-linear frequency domain method [18], which, when used in its original form, requires a large non-linear set of equations to be solved in an iterative way. This proves to be unpractical for most modal data sets hence alternative methods have been developed. Below, two prominent ones are presented. The discussed methods are applicable to both FRFs (input-output data) and output-only spectra (operational data).

#### 3.1 LSCE

The still most widely used approach is the Polyreference Least Squares Complex Exponential (LSCE) method which dates from the early 80s [19]. The method starts from the Impulse Responses (IR) between the measured inputs and outputs and yields global estimates of poles and the modal participation factors.

Define the impulse response function matrix  $[h_k]$  at time instant  $k$  between  $N_{\text{resp}}$  responses and  $N_{\text{ref}}$  inputs. Mathematically, the Polyreference LSCE will decompose the correlation functions as a sum of decaying sinusoids. So,

$$[h_k] = \sum_{r=1}^{N_m} \{\psi\}_r e^{\lambda_r k \Delta t} \{L\}_r^T + \{\psi\}_r^* e^{\lambda_r^* k \Delta t} \{L\}_r^{T*} \quad \text{or} \quad (3)$$

$$[h_k] = \sum_{r=1}^{N_m} \{\psi\}_r \mu_r^k \{L\}_r^T + \{\psi\}_r^* \mu_r^{k*} \{L\}_r^{T*}$$

where system pole  $\mu_r = e^{\lambda_r \Delta t}$  and  $\{L\}_r$  is a column vector of  $N_{\text{ref}}$  modal participation factors, which are multipliers which are constant for all response stations for the  $r$ -th mode. The combinations of complex exponential and constant multipliers,  $\mu_r \{L\}_r^T$  or  $\mu_r^* \{L\}_r^{T*}$  are a solution of the following matrix finite difference equation of order  $t$ :

$$\mu_r^k \{L\}_r^T [I] + \mu_r^{k-1} \{L\}_r^T [W]_1 + \dots + \mu_r^{k-t} \{L\}_r^T [W]_t = \{0\}^T \quad (4)$$

where  $[W]_1 \dots [W]_t$  are coefficient matrices with dimension  $N_{\text{ref}} \times N_{\text{ref}}$ . In case the system has  $N_m$  physical modes, the order  $t$  in equation (4) has to be greater than or equal to  $2N_m/N_{\text{ref}}$ .

Since the impulse response functions are a linear combination of the characteristic solutions of equation (4),  $\mu_r \{L\}_r^T$  or  $\mu_r^* \{L\}_r^{T*}$ , they are also a solution of that equation. Hence,

$$[h_k][I] + [h_{k-1}][W]_1 + \dots + [h_{k-t}][W]_t = [0] \quad (5)$$

Equation (5) uses all response stations simultaneously enabling a global least squares estimate of the coefficient matrices  $[W]_1 \dots [W]_t$ . Overdetermination is achieved by considering all available or selected time intervals. Once the coefficient matrices are known, equation (4) can be reformulated into a generalized Eigenvalue problem resulting into  $N_{\text{ref}} t$  Eigenvalues  $\mu_r$ , as estimates for the system poles  $\lambda_r$  and the corresponding left eigenvectors  $\{L\}_r^T$ .

As the Polyreference LSCE does not yield the mode shapes, a second step is needed to extract these using the identified modal frequencies, damping ratios and participation factors as known parameters in equation (1), which now becomes a simple linear set of equations.

## 3.2 PolyMAX

As stated before, the highly interactive pole-selection requires a large user experience. A major research topic has hence been the development of system identification algorithms with improved stabilization behavior. Impressive results are for example obtained with the recently developed ‘‘Least Squares Complex Frequency Domain (LSCF)’’ method [20, 21]. This discrete frequency domain method uses a least squares or total least squares approach to fit a rational fraction polynomial model to a MIMO FRF matrix. Originally a common-denominator model structure was used. Recently a right matrix-fraction variant of the method was introduced. In this so-called ‘‘PolyMAX’’ method, following model is identified from the FRF data:

$$[H(\omega)] = \sum_{r=0}^p z^r [\beta_r] \cdot \left( \sum_{r=0}^p z^r [\alpha_r] \right)^{-1} \quad (6)$$

where  $[\beta_r] \in \mathbb{C}^{l \times m}$  are the numerator matrix polynomial coefficients,  $[\alpha_r] \in \mathbb{C}^{m \times m}$  are the denominator matrix coefficients, and  $p$  is the model order. Note that a so-called  $z$ -domain model (i.e. frequency-domain model that is derived from a discrete-time model) is used in (6), with:

$$z = e^{j\omega \Delta t} \quad (7)$$

where  $\Delta t$  is the sampling time. Equation (6) can be written down for all values  $\omega$  of the frequency axis of the FRF data. Basically, the unknown model coefficients  $[\alpha_r]$ ,  $[\beta_r]$  are then found as the least-squares solution of these equations (after linearization). More details can be found in [22, 23].

Very high system orders (over 50) are clearly identified in a single-step procedure, leading to extremely clear stabilization diagrams, and hence drastically improving the quality and the interpretability of the result. It is a feature of the PolyMAX identification method to estimate the mathematical poles with negative damping ratio. Hence these poles are readily excluded before constructing the stabilization diagram. The fact that inherently unstable models are identified is not a problem as a new model is recomposed after selection of the stable poles from the stabilization diagram.

#### 4 Proof-of-Concept: The Modal Analysis Chain

In [2, 3], a rule-based approach is presented that identifies the steps and the knowledge used by an expert engineer assessing a stabilization diagram. This implicit knowledge was then made explicit by casting it into rules. In short, the engineer visually inspects the symbols in the stabilization diagrams, which are based on similarity in frequency, damping ratio and/or mode vectors between poles belonging to subsequent model orders. Based on these sources of information, the engineer selects a number of poles by hand. In a later step, this pole selection is checked with validation criteria (Section 5).

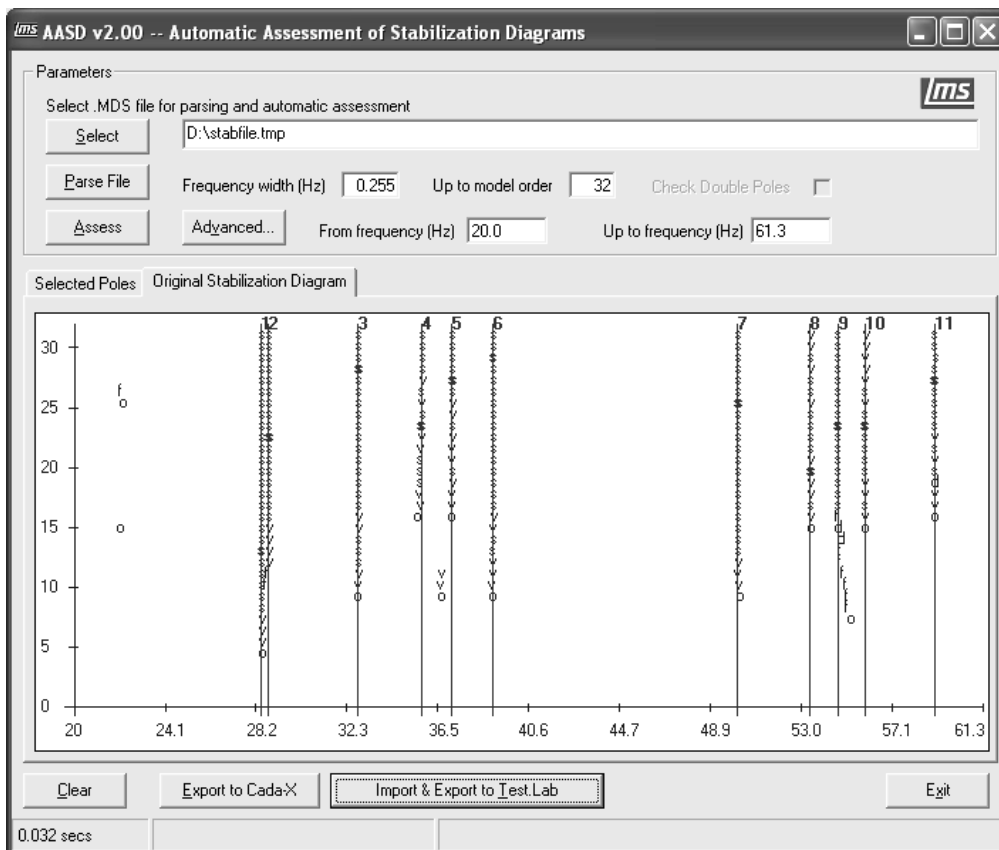


Figure 1: Screenshot AASD: Automatic Assessment of Stabilization Diagrams.

The original tool that was created from this, AASD (Automatic Assessment of Stabilization Diagrams), allows to select a stabilization diagram file that was exported from LMS Cada-X software, perform the automatic pole-selection, and finally import this selection back into Cada-X (figure 1).

The successor of Cada-X, LMS Test.Lab<sup>TM</sup> provides valuable technology that made it possible to fully integrate the AASD tool in the Modal Analysis application. Using Windows Automation it is possible for external applications to communicate and interact with Test.Lab. The AASD tool now grabs a generated stabilization diagram from the Test.Lab Modal Analysis application and performs the automatic assessment. When finished, it passes the resulting pole-selection back to Test.Lab, as if the selection was done by hand

(figure 2). The user can then assess the resulting mode shapes to his/her own judgement, and proceed to the validation step.

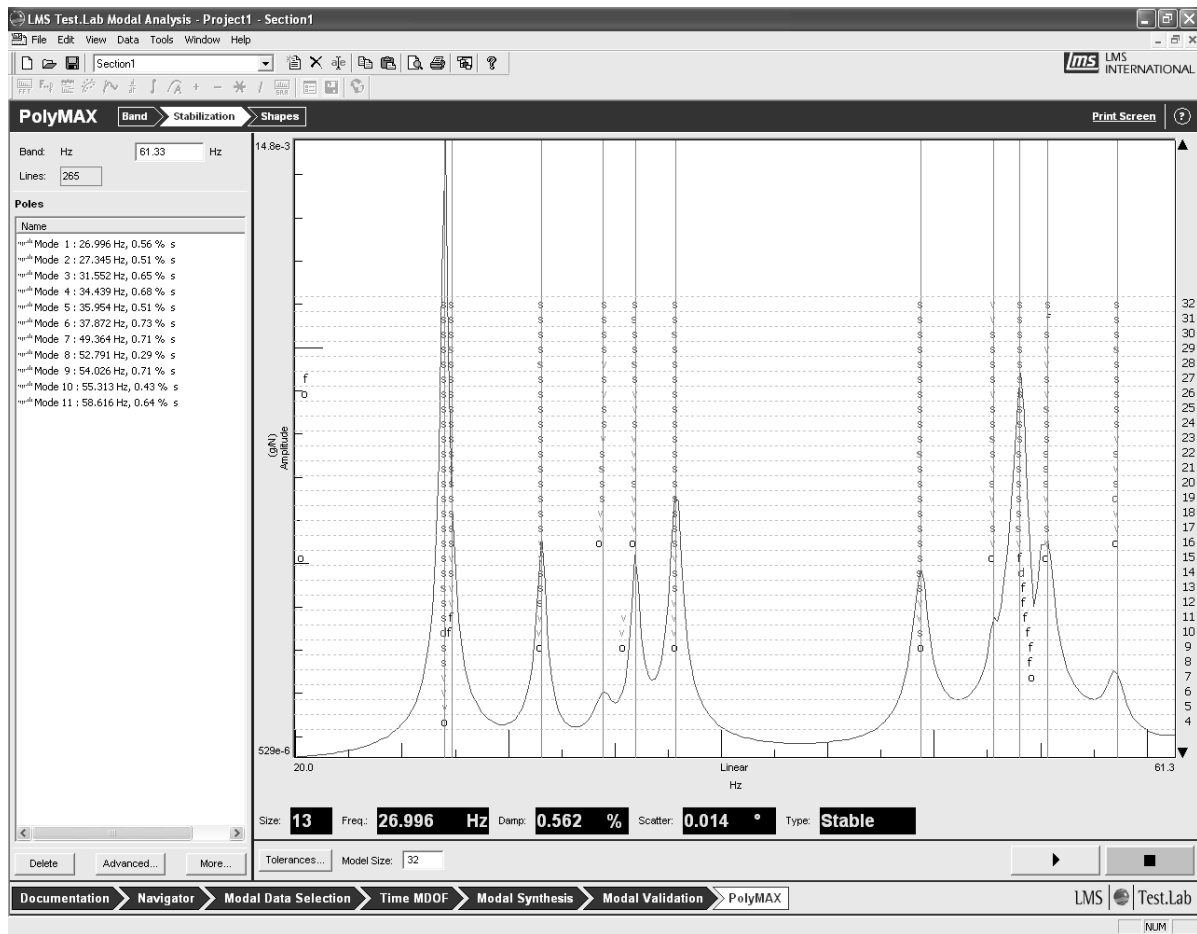


Figure 2: Test.Lab Modal Analysis: PolyMAX Stabilization sheet. Pole selection by AASD.

## 5 Validation Criteria

A number of validation criteria exist that can be used to determine the quality of a parameter estimation of mode shapes. The criteria presented below will be used in the benchmark test, section 6.

- **Synthesized vs. Measured FRFs/spectra:** Test.Lab uses the selected modes to synthesize the measured FRFs/spectra. The higher the correlation with the corresponding measured FRFs/spectra, the better the modal model. A criterion that can be used for this is the Complex Mode Indicator Function (CMIF), where the FRFs/spectra are compressed by using their 3 principal components.
- **Modal Phase Collinearity (MPC):** The MPC is an indicator that checks the degree of complexity of a mode [5]. It evaluates the functional linear relation between the real and imaginary parts of the mode shape coefficients. In general, for true physical modes the MPC value approaches 1, whereas low values indicate again noisy or computational modes.
- **Mean Phase Deviation (MPD):** The MPD is another statistical indicator of the complexity of a mode shape [5]. The MPD expresses the phase scatter of each mode shape. For true physical mode shapes, its value is 0.

## 6 Benchmark Test

The goal of the benchmark test is to give a qualitative assessment of the AASD tool, and to place it within the spectrum of novice to experienced modal analysts. A group of 8 people was selected for this, containing 4 novices, and 4 experts, all with an engineering background. Two data sets were selected, both analyzed with two parameter estimation methods, leading in total to four stabilization diagrams (Figures 3, 4, and 5). Note the clean PolyMAX stabilization diagrams. The novices received a short description of the task they had to carry out:

1. *The stabilization diagram shows poles – solutions of a mathematical problem – at different model orders. The task of the engineer is to select an – unknown – number of poles at different frequencies. Occurrence of a pole at the same frequency at increasing model orders gives the engineer information on the physical correspondence of this pole.*
2. *First, the engineer will look for a vertical column of poles. Especially if this column will contain lots of s-type (and d-type) poles. It is not important that this column should exist at the lower model orders, nor that it is a straight column at the lower orders.*
3. *Next the engineer inspects the s-type and d-type poles in particular, in which he values the s-type poles more than the d-type poles. The engineer searches for the pole in the column that is the most stable in frequency and which stabilizes in damping and scatter at a certain order.*

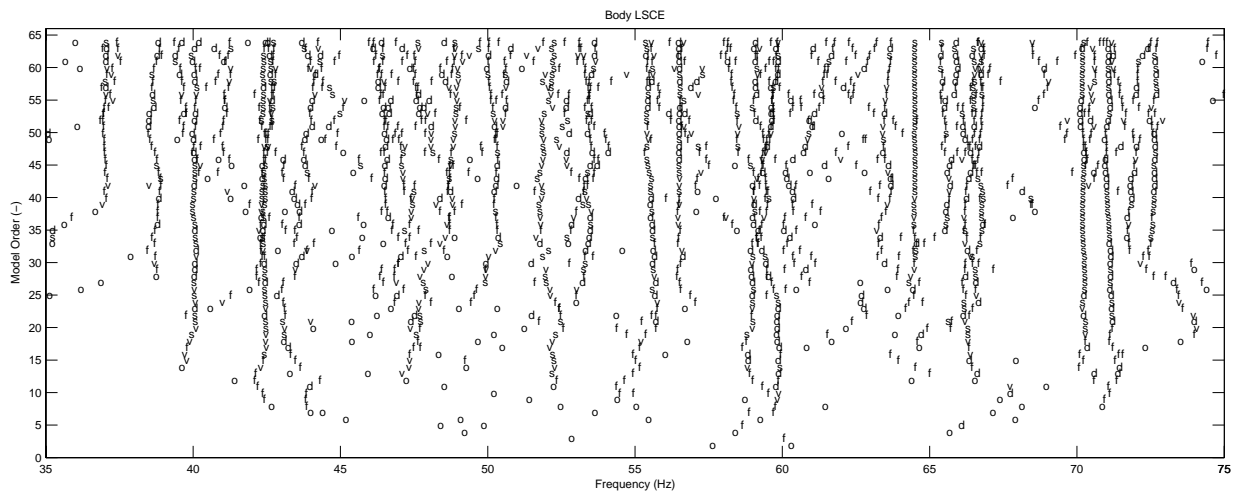


Figure 3: Stabilization diagram for Body data, analyzed with LSCE.

The first data set is a multiple-input multiple-output (MIMO) data set from the body of a car. It has 2 inputs and 264 measurement points all over the car body, leading to 528 FRFs. The parameter estimation was done with both a time domain method (LSCE) and a frequency domain method (PolyMAX) for the frequency band 35–75Hz. Both stabilization diagrams were created to a model size of 64.

The second data set is an output-only data set, from an in-flight test of an aircraft. During the measurements, no artificial excitation was applied. The plane was just excited by atmospheric turbulence, which cannot be measured, but is assumed to be white noise. It has 3 reference points and 7 outputs from various points all over the airplane, leading to 21 spectra. The parameter estimation was done again with both an operational time domain method – Balanced Realization, BR, which is a subspace identification method [4][24] – and a frequency domain method (Operational PolyMAX) for the frequency band 0.50–2.26Hz. This may sound strange for an in-flight data set, but the data was rescaled due to a non-disclosure agreement with the data

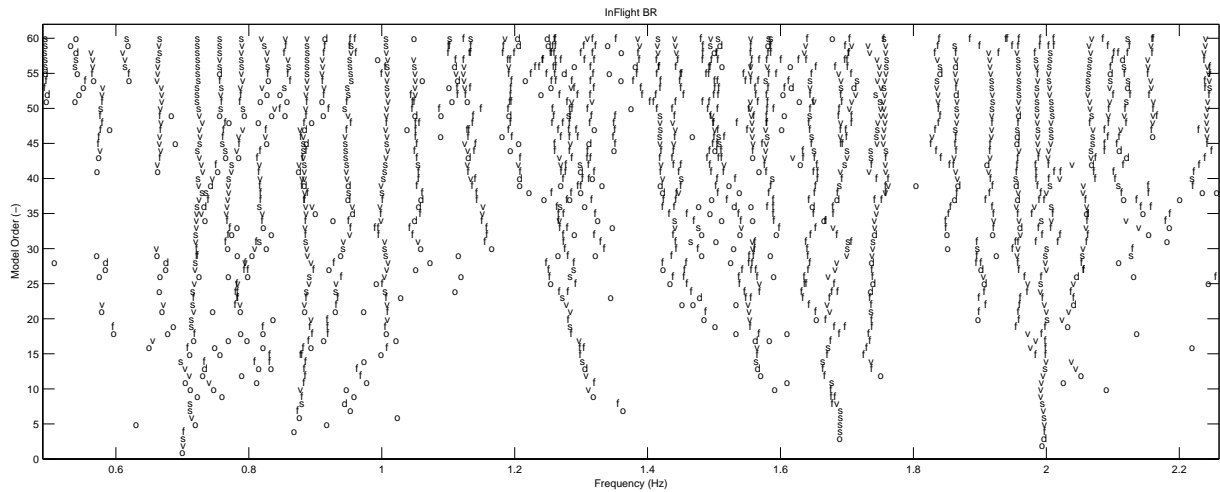


Figure 4: Stabilization diagram for InFlight data, analyzed with BR.

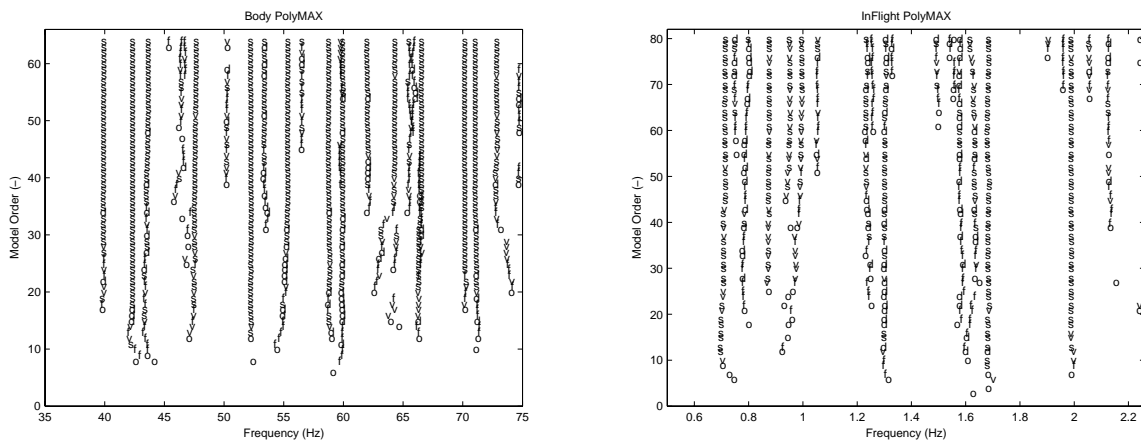


Figure 5: Stabilization diagrams for Body and InFlight data, both analyzed with PolyMAX.

provider. The BR diagram was created up to a model size of 60, whereas the PolyMAX diagram was created up to model size 80.

## 6.1 Observations

A first observation of the stabilization diagrams showed that the LSCE/BR stabilization diagrams – the former standard – were quite complicated, whereas the PolyMAX diagrams were quite clear, showing clear poles – and only clear poles – throughout the whole frequency band. This resulted in large differences in the number of selected poles by the different test subjects. Figure 6 shows the distribution of the number of selected poles of the 4 stabilization diagrams. The dark bar represents the bar in which the AASD results are included. A first observation is that in general, the AASD tool is always in the high end of this spectrum, suggesting an overestimate of the number of poles.

Also the time of the assessment was measured. In general the LSCE/BR tasks took about twice as much time as the PolyMAX tasks. Next to that, the experts spent about twice as much time in the assessment as the novices. The novices were quite overwhelmed by the complexity of the LSCE/BR diagrams, in which they quickly gave up. AASD assessment takes only a few seconds (<10sec).

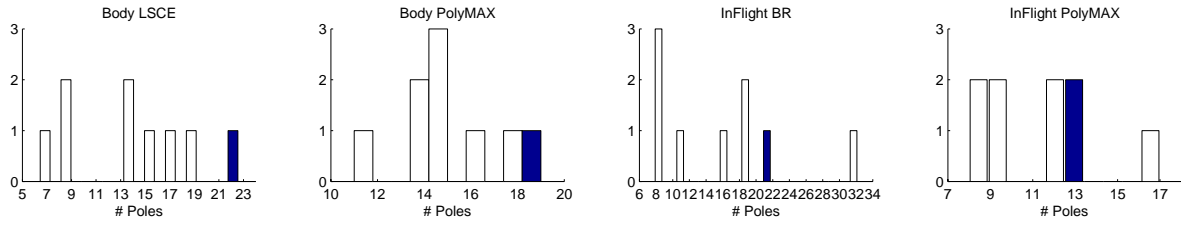


Figure 6: Distribution of the number of selected poles per user for the 4 different stabilization diagrams.

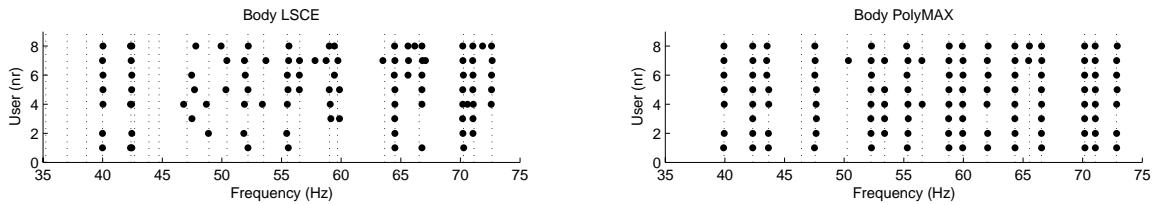


Figure 7: Body LSCE and PolyMAX pole selection per user.

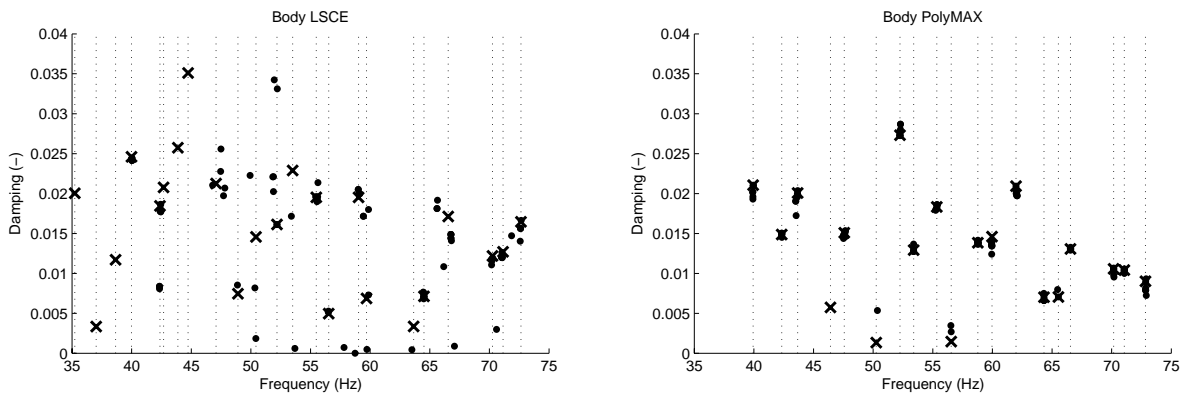


Figure 8: Body LSCE and PolyMAX pole selection, frequency vs. damping.

Figure 7 shows a frequency spectrum of the pole selection of all the test subjects on the two body stabilization diagrams. Users 1–4 are the novices, where users 5–8 are the experts. The vertical dotted lines show the selection made by the AASD tool. The LSCE diagram clearly shows that the novices had a hard time in the 45–60Hz band. A majority of the experts select poles at about the same frequencies as AASD, but the alignment is not that nice. AASD selects 5 poles that have not been selected by any of the test subject but almost all of the other poles are also selected by a majority of the experts. In one case at about 42.5Hz, the test subjects have selected one pole, where AASD has selected two. This means that the users feel that two branches at a lower order have stabilized into one pole, whereas AASD has found enough evidence to mark them as separate poles. Finally, at 65.6Hz a majority of the experts have selected a pole that was missed by AASD and all the novices.

In the PolyMAX diagram, AASD has selected two poles that no (or hardly any) subject has selected. There are two poles that were selected by only two test subjects. All other poles were also selected by a big majority.

Next, the damping of the selected poles is compared, and presented in figure 8. The crosses represent the AASD selection. A cluster of dots represents consensus over the selection by the different test subjects, whereas a scatter over the damping would indicate indecisiveness. In general the users have more consensus with respect to damping in the PolyMAX diagram than in the LSCE diagram. AASD largely agrees with this consensus. The differences are explained by the sparse number of selections on the 45–60Hz band. Remarkable is the improvement for both novices and experts in that band in the PolyMAX plot.

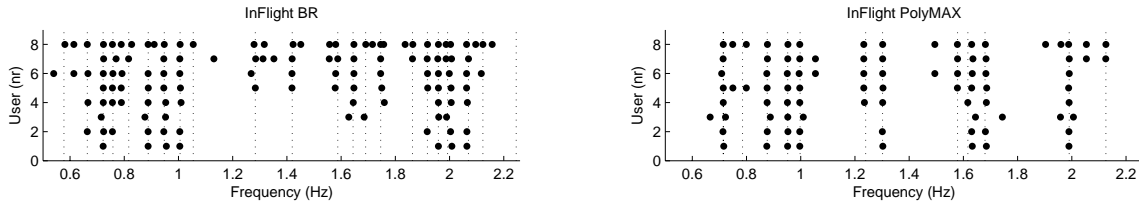


Figure 9: InFlight BR and PolyMAX pole selection per user.

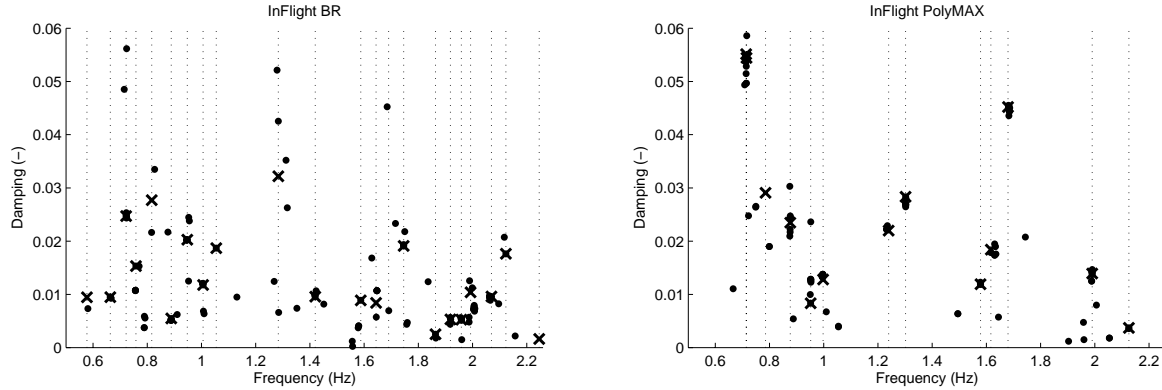


Figure 10: InFlight BR and PolyMAX pole selection, frequency vs. damping.

Figure 9 shows the frequency spectrum again of the pole selection of all the test subjects but now on the two in-flight stabilization diagrams. Users 1–4 are the novices again, and users 5–8 are the experts. The vertical dotted lines show the selection made by the AASD tool. Most remarkable is the trouble that the novices had in the 1.0–1.6 Hz band, where the experts agree with AASD. Overall, a majority of the experts select poles at the same frequencies as AASD. Next, there are 3 AASD poles that were hardly selected by any of the test subjects, and four poles that were only selected by two subjects.

In the PolyMAX diagram, there is a big consensus over almost all the poles. This time there is no significant difference between novices and experts. There are two poles that are next to AASD only selected by two expert test subjects. Next there are three poles that have not been selected by AASD, but only by two experts.

Figure 10 shows the damping of the selected poles. The crosses represent again the AASD selection. In general the users have again more consensus with respect to damping in the PolyMAX diagram than in the BR diagram. In analogy to the body stabilization diagrams, the AASD poles fit also nicely in the consensus clusters of the test subjects. The exceptions in the BR diagram and in the PolyMAX diagram correspond to the previously discussed poles that were hardly selected by the test subjects.

## 6.2 Using Validation Criteria

Typically the differences between measured and synthesized FRFs or spectra are used to assess the validity of a modal model (see Section 5). As an example, this validation criterion is applied to the subspace identification results of the in-flight data. In Figure 11, the measured cross spectra are compared with the cross spectra synthesized from the identified modal parameters. The information of 21 ( $7 \times 3$ ) spectra is compressed by using their 3 principal components (also called CMIF in modal analysis). The left figure is the result of a novice, selecting only a few modes; the right one represents the AASD results, which are very close to the results of the expert users. The main conclusion is that AASD is able to successfully extract the relevant dynamic information from the in-flight data.

This criterion has to be applied with some care as it is well known that the fit always improves when more parameters are included in the model. Figure 12 shows the correlation between the 3 CMIFs computed from

the measurement data and the CMIFs computed from the identified modal model. As it is typical that the correlation increases with an increasing number of modes, there is only a marginal improvement after 20 modes. The fact that the correlation is not uniformly increasing with an increasing number of modes can be explained by the human factor: some subjects reached a better correlation with less modes due to a better selection.

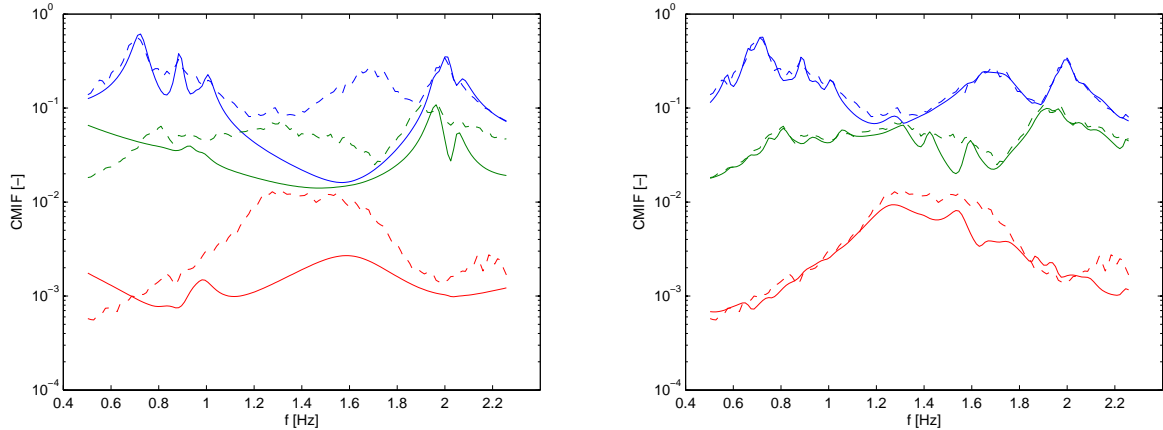


Figure 11: CMIF plots of in-flight BR data set for worst novice fit (left) and AASD close to best fit (right).

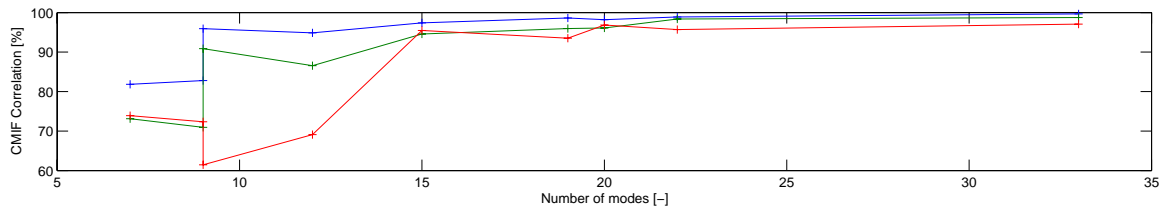


Figure 12: CMIF correlation plot for increasing number of modes for in-flight BR data set.

For a discussion on the Modal Phase Collinearity (MPC) and Modal Phase Deviation (MPD) criteria, the pole selection is used that was retrieved from the body data set using the LSCE method, as well as the InFlight PolyMAX diagram. First, a set of poles was constructed on which there seemed to be consensus based on observation. This can be visually validated by observing figure 3. Next, all the MPC and MPD values for those poles were calculated. In order to compare the AASD tool with the novices and the experts, average values were taken for each category. If a test subject did not select a pole, this was not included in the average. The results are presented in table 1. Note that high MPC values as well as low MPD values indicate physical poles.

AASD has a better MPC than the experts for 5 out of the 9 consensus poles, and has a better MPC than the novices for 6 out of 9 consensus poles. AASD has 2 poles for which it scores remarkably low. In the case of pole 5 at 42.4Hz, the diagram of figure 8 shows us that AASD has considered 2 poles there, where the experts and novices have considered only 1. AASD has probably selected 2 poles at a low model order that reflect the same physical phenomenon, but have not yet stabilized. The score of the experts and the novices show that there is evidence for the existence of a physical pole at that frequency. The other remarkable pole is pole 19 at 64.5Hz. Besides a low MPC for AASD, the novices and also the experts only reach a MPC of about 60%. Inspecting the mode shape animation showed that this mode is indeed a complex mode but still physically meaningful, where in general, true physical modes not do have complex shapes. Note that trimmed car bodies sometimes have complex mode shapes due to local damping effects.

There remains one remarkable MPC value for the novices: they completely missed pole 15 at 56.5Hz, which was situated at the edge of the difficult frequency band 45–60Hz. The MPD values in table 1 show exactly the same result as the MPC values. The high values for AASD for poles 5 and 19 reflect the previous discussion. Table 2 shows the MPC and MPD values for the InFlight data set and the PolyMAX stabilization diagram.

pole #	Freq[Hz]	Damp[%]	MPC [%]			MPD [deg]		
			AASD	Avg.Nov.	Avg.Exp.	AASD	Avg.Nov.	Avg.Exp.
4	40.0	2.46%	93	86	88	17	23	21
5	42.4	1.85%	<b>32</b>	77	86	<b>62</b>	33	24
14	55.5	1.95%	81	61	71	29	46	38
15	56.5	0.50%	81	-	70	29	-	38
19	64.5	0.71%	<b>37</b>	62	62	<b>61</b>	43	45
20	66.6	1.71%	80	79	81	34	39	31
21	70.3	1.22%	98	82	96	10	29	13
22	71.1	1.27%	95	89	88	14	22	22
23	72.6	1.65%	70	76	77	40	36	33

Table 1: MPC and MPD: Body with LSCE, split into AASD, Average Novices, and Average Experts.

pole #	Freq[Hz]	Damp[%]	MPC [%]			MPD [deg]		
			AASD	Avg.Nov.	Avg.Exp.	AASD	Avg.Nov.	Avg.Exp.
1	0.71	5.51%	<b>81</b>	99	100	<b>34</b>	6	4
3	0.78	2.91%	68	75	72	37	32	34
4	0.88	2.35%	80	80	83	27	28	25
5	0.95	0.83%	95	96	97	15	12	13
6	1.00	1.28%	95	89	92	19	26	26
7	1.24	2.20%	96	98	95	11	7	11
8	1.30	2.83%	94	-	90	20	-	25
9	1.58	1.19%	<b>96</b>	85	79	<b>13</b>	25	30
10	1.62	1.84%	98	99	99	10	7	6
11	1.68	4.52%	100	100	100	1	2	3

Table 2: MPC and MPD: InFlight with PolyMAX, split into AASD, Average Novices, and Average Experts.

A first observation is that the novices performed equally well as the experts, sometimes even slightly better, even though they all missed pole 8 at 1.30Hz. The second observation is that AASD performs poorly on pole 1. The MPC is more or less acceptable, but the MPD is really bad, especially compared with the scores of the experts and novices. However, on pole 6 and 9, AASD has a significantly better MPD value than both experts and novices, and also the MPC is much better.

In general, it can be said that the novices score equally well on the PolyMAX diagram as the experts do. Apart from pole 1, AASD also performs at or sometimes above the level of the experts.

## 7 Conclusions

One of the first observations was that AASD selects a rather high number of poles, as do the experts. It can be concluded however, that this does not seem to impact the results, as pointed out by the validation criteria CMIF, MPC, and MPD.

Next, the results showed that for difficult stabilization diagrams, acquired from parameter estimation methods like LSCE or BR, the quality of the AASD selection meets those made by the experts rather than those made by the novices. For clean PolyMAX stabilization diagrams, the tool and also the novices(!) perform at least equally well as the experts. This supports the statement that PolyMAX yields user-independent results.

Finally, it has to be said that computationally, AASD by far outperforms human users in the order of seconds versus minutes. We therefore suggest that the AASD tool will have an advisory role in the modal analysis chain, with the adagio ‘no gain no pain’. Both expert and novices could then start off with the AASD selection, and make changes when they think this is needed, thereby saving valuable time. For applications such as on-line flutter monitoring, this could also prove to be a valuable automation step.

Based on this research, we recommend as an improvement for AASD that it also uses validation criteria to assess its own selection. The heuristic that complex modes do not tend to be physical modes could be implemented using the MPC/MPD validation criteria. This could however also lead to an elimination of complex modes, that still are true physical modes, like in the Body/LSCE case.

Also, depending on the expertise of the user the tool could be fine-tuned to user scenarios, such as:

- Overestimation: focussing on recall (percentage of the total number of physical poles found)
- Underestimation: focussing on precision (percentage of selected poles that are also physical)
- A mix of these two

At this moment, AASD tends to be tuned to overestimate, thereby focussed on not missing any poles, which could be well suited for experts because they have the expertise to remove poles that they feel are not physical.

## 8 Acknowledgement

This work was carried out in the frame of the EC research project NMP2-CT-2003-501084 “INMAR” (Intelligent Materials for Active Noise Reduction); see also <http://www.lbf.fhg.de/inmar>. The support of the EC is gratefully acknowledged.

## References

- [1] Van der Auweraer, H. and Peeters, B. Discriminating physical poles from mathematical poles in high order systems: Use and automation of the stabilization diagram. *Proc. of IMTC2004, the 21th IEEE Instrumentation and Measurement Technology Conf., Como, Italy*, pages 2193–2198, 2004.
- [2] Lanslots, J. and Scionti, M. Automatic Assessment of Stabilization Diagrams. Technical Report, LMS International, TST Research & Technology Development, Leuven, Belgium, 2002.
- [3] Scionti, M., Lanslots, J., Goethals, I., Vecchio, A., Van der Auweraer, H., Peeters, B., and De Moor, B. Tools to Improve Detection of Structural Changes from In-Flight Flutter Data. *Proc. of the VIII Int. Conf. on Recent Advances in Structural Dynamics, Southampton, U.K.*, 2003.
- [4] Peeters, B. System Identification and Damage Detection in Civil Engineering. Ph.D. Thesis, Dep. of Civil Eng., K.U. Leuven, Belgium, <http://www.bwk.kuleuven.ac.be/bwm>, 2000.
- [5] Heylen, W., Lammens, S., and Sas, P. *Modal Analysis Theory and Testing*. Katholieke Universiteit Leuven, Department of Mechanical Eng., PMA, Leuven (Heverlee), Belgium, 1997.
- [6] Verboven, P., Parloo, E., Guillaume, P., and Van Overmeire, M. Autonomous structural health monitoring – part i: modal parameter estimation and tracking. *Mechanical Systems and Signal Processing*, 16(4):637–657, 2002.
- [7] Verboven, P., Guillaume, P., Cauberghe, B., Parloo, E., and Vanlanduit, S. Stabilization charts and uncertainty bounds for frequency-domain linear least squares estimators. *Proc. of IMAC 21, the Int. Modal Analysis Conf., Kissimmee, Florida, USA*, pages 637–657, 2003.
- [8] Chhipwadia, K.S., Zimmerman, D.C., and James III, G.H. Evolving autonomous modal parameter estimation. *Proc. of IMAC 17, the Int. Modal Analysis Conf., Kissimmee, Florida, USA*, pages 819–825, 1999.

- [9] Goethals, I. and De Moor, B. Subspace identification combined with new mode selection techniques for modal analysis of an airplane. *Proc. of SYSID-2003, the 13th IFAC Symposium on System Identification, Rotterdam, The Netherlands, 2003.*
- [10] Pappa, R.S., James III, G.H., and Zimmerman, D.C. Autonomous model identification of the space shuttle tail rudder. *Journal of Spacecraft and Rockets*, 35(2):163–169, 1998.
- [11] Juang, J.-N. and Pappa, R. An eigensystem realization algorithm for modal parameter identification and reduction. *Journal of Guidance, Control and Dynamics*, 8(5):620–627, 1985.
- [12] Verboven, P., Parloo, E., Guillaume, P., and Van Overmeire, M. Autonomous modal parameter identification based on a statistical frequency-domain maximum likelihood approach. *Proc. of IMAC 19, the Int. Modal Analysis Conf., Kissimmee, Florida, USA*, pages 1511–1517, 2001.
- [13] Vanlanduit, S., Verboven, P., Schoukens, J., and Guillaume, P. An automatic frequency domain modal parameter estimation algorithm. *Proc. of Int. Conf. on Structural System Identification, Kassel, Germany*, pages 637–646, 2001.
- [14] Goethals, I. and De Moor, B. Model reduction and energy analysis as a tool to detect spurious modes. *Proc. ISMA 2002, the Int. Conf. on Noise and Vibration Eng., Leuven, Belgium*, pages 1307–1314, 2002.
- [15] Lanslots, J., Scionti, M., and Vecchio, A. Fuzzy Clustering Techniques to Automatically Assess Stabilization Diagrams. *Proc. of the 7th Int. Conf. on the Application of Artificial Intelligence to Civil and Structural Eng., Egmond-aan-Zee, The Netherlands*, paper 46, 2003.
- [16] Van Overschee, P. and De Moor, B. *Subspace identification for linear systems: theory, implementation, applications*. Kluwer Academic Publishers, Dordrecht, The Netherlands, 1996.
- [17] Leuridan, J. Some direct parameter model identification methods applicable for multiple input modal analysis. Ph.D. Thesis, Univ. of Cincinnati, USA, 1984.
- [18] Busturia, J. and Gimenez, J. Multi-excitation multi-response non-linear least squares algorithm. *Proc. of 10th ISMA, the Int. Conf. on Noise and Vibration Eng., Leuven, Belgium*, 1985.
- [19] Vold, H., Kundrat, J., Rocklin, T., and Russel, R. A multi-input modal parameter estimation algorithm for mini-computers. *SAE paper 820194, Trans. SAE*, 91(1):815–821, 1982.
- [20] Guillaume, P., Verboven, P., and Vanlanduit, S. Frequency-domain maximum likelihood identification of modal parameters with confidence intervals. *Proc. ISMA 23, the Int. Conf. on Noise and Vibration Eng., Leuven, Belgium*, 1998.
- [21] Van der Auweraer, H., Guillaume, P., Verboven, P., and Vanlanduit, S. Application of a fast-stabilizing frequency domain parameter estimation method. *ASME Journal of Dynamic Systems, Measurement, and Control*, 123(4):651–658, 2001.
- [22] Guillaume, P., Verboven, P., Vanlanduit, S., Van der Auweraer, H., and Peeters, B. A poly-reference implementation of the least-squares complex frequency-domain estimator. *Proc. of IMAC 21, the Int. Modal Analysis Conf., Kissimmee, FL, USA*, 2003.
- [23] Peeters, B., Guillaume, P., Van der Auweraer, H., Cauberghe, B., Verboven, P., and Leuridan, J. Automotive and aerospace applications of the polymax modal parameter estimation method. *Proc. of IMAC 22, the Int. Modal Analysis Conf., Dearborn, MI, USA*, 2004.
- [24] Hermans, L. and Van der Auweraer, H. Modal testing and analysis of structures under operational conditions: industrial applications. *Mechanical Systems and Signal Processing*, 13(2):193–216, 1999.